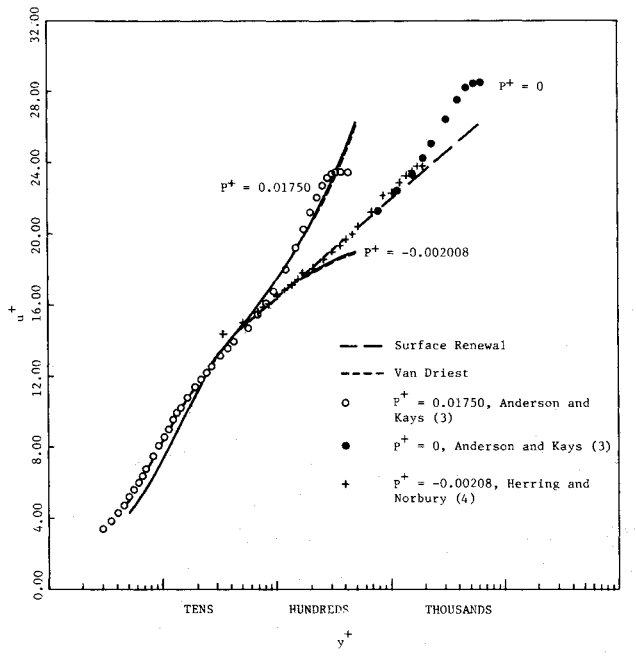

Fig. 2 Comparison of calculations for u^+ with experimental data.

the latter approach is used. Calculations obtained for s^+ and y_M^+ by coupling Eqs. (6) and (8) and matching the solution with representative experimental data[3] within the intermediate region are shown in Fig. 1. The analysis indicates a slight increase in s^+ and a moderate decrease in y_M^+ for increasing values of P^+ in the range $-0.01 \lesssim P^+ \lesssim 0.02$. The calculations for s^+ and y_M^+ are correlated to within 1% for $-0.01 \lesssim P^+ \lesssim 0.02$ by

$$s^+ = 0.004319(1 + aP^+) \tag{11}$$

where $a = 0.342$ for $P^+ > 0$ and $a = 7.5$ for $P^+ < 0$, and

$$y_M^+ = 44 - 910P^+, \qquad P^+ \leq 0 \tag{12a}$$

$$= 30 + 14\exp(-35P^+), \qquad P^+ \geq 0 \tag{12b}$$

Calculations for u^+ obtained using Eqs. (6) and (8-12) are compared with experimental data[3,4] in Fig. 2. Calculations obtained using the damping factor approach with a^+ specified as a function of P^+ by the correlation developed by Anderson et al.[3] are also shown in Fig. 2. The surface renewal and damping factor calculations for u^+ are essentially identical in the region for which $y^+ \gtrsim 20$. However, Eq. (8) lies moderately below the damping factor calculations and the experimental data for $y^+ \lesssim 20$, with a maximum difference of about 14% occurring at $y^+ = 7$. This difference, which is of no practical consequence in the analysis of the mean flowfield for turbulent boundary-layer flows, is primarily caused by the simplifying approximation $\bar{U}_I = \bar{U}_{Ic}$.

Conclusion

The present analysis demonstrates the usefulness of the surface renewal model for characterizing the wall region for fully turbulent boundary-layer flow with pressure gradients. The simple analytical relationship given by Eq. (8) expresses u^+ within the wall region in terms of the dimensionless burst frequency s^+ which is correlated in terms of P^+ by Eq. (11). When coupled with the classical mixing-length representation given by Eq. (6), the model predictions are essentially equivalent to results obtained by the damping factor method and are in good agreement with experimental data within the Couette flow region for adverse and favorable pressure gradients. The surface renewal inner law is readily incorporated into numerical codes by using Eq. (8) within the wall region, beginning the computational grid at y_M^+ and using the defining relations $u^+ = \bar{u}/U^*$ and $y^+ = yU^*/\nu$. The moderate underprediction of u^+ with the region $y^+ \lesssim 20$ is a result of the simplifying approximation $\bar{U}_I = \bar{U}_{Ic}$. Although the difference between Eq. (8) and the data in this region is of no practical consequence for this application, the effect of the unreplenished layer of fluid at the surface is significant for turbulent boundary-layer flows with blowing and heat and mass transfer. The more general surface rejuvenation model[5] provides a basis for analyzing these transport processes and for obtaining more accurate calculations within the close vicinity of the wall for pressure gradient flows.

Acknowledgment

Support provided for this study by the University of Petroleum and Minerals is gratefully acknowledged.

References

[1]van Driest, E. R., "On Turbulent Flow Near a Wall," *Journal of the Aeronautical Sciences*, Vol. 23, 1956, pp. 1007-1011.

[2]Thomas, L. C., "A Turbulence Burst Model of Wall Turbulence for Two-Dimensional Turbulent Boundary Layer Flow," *International Journal of Heat and Mass Transfer*, Vol. 25, 1982, pp. 1127-1136.

[3]Anderson, P. S., Kays, W. M., and Moffat, R. J., "Experimental Results for the Transpired Turbulent Boundary Layer in an Adverse Pressure Gradient," *Journal of Fluid Mechanics*, Vol. 69, 1975, pp. 353-375.

[4]Herring, H. and Norbury, J., "Some Experiments on Equilibrium Turbulent Boundary Layers in Favorable Pressure Gradients," *Journal of Fluid Mechanics*, Vol. 27, 1976, pp. 541-549.

[5]Thomas, L. C., "The Surface Rejuvenation Model of Wall Turbulence: Inner Laws for u^+ and T^+," *International Journal of Transfer*, Vol. 23, 1980, pp. 1097-1104.

Experimental Study of Surface Pressure in Three-Dimensional Turbulent Jet/Boundary Interaction

Christos D. Tsitouras* and Latif M. Jiji†
The City College of the City University of New York
New York, New York

Introduction

IT is well known that the presence of a boundary in the vicinity of a jet has a significant effect on the jet's behavior. Examples of jet/boundary interaction problems include impinging, wall, and offset jets. In the impinging jet, the fluid stream is directed toward a surface. In the wall jet, it is discharged parallel to and along a surface. In the offset jet, the fluid is discharged parallel to a surface from a nearby outlet (see Fig. 1). Clearly, the wall jet is a limiting case of the offset jet.

Although two-dimensional offset jets have been extensively investigated, little is known about three-dimensional offset jets. In this Note, we examine three-dimensional turbulent offset jets discharged from rectangular channels parallel to a

Received March 22, 1985; revision submitted Oct. 24, 1985.

*Graduate Student, Mechanical Engineering Department. Member AIAA.

†Herbert Kayser Professor, Mechanical Engineering Department. Member AIAA.

plane surface. See Fig. 1. Particular attention is focused on the surface pressure distribution resulting from this type of jet/boundary interaction. This configuration was examined by Sacks et al.[1] using slender rectangular outlets of small aspect ratios, $e=d^*/\ell^*=0.02$ and 0.04 at various offset distances $h=h^*/d^*$. They obtained surface pressure data that were limited to measurements along the lateral condinate x_3^* at a single axial distance x_1^* by using a discharge aspect ratio $e=0.02$ at two different offset positions. Based on velocity measurements and flow visualization, Sacks et al.[1] demonstrated that the three-dimensional offset jet, even for very slender outlets, differs significantly from its two-dimensional counterpart: 1) flow recirculation characterizing two-dimensional offset jets in the preattachment region near the discharge does not occur in three-dimensional jets; and 2) the preattachment region of three-dimensional jets is dominated by induced cross flow that is not present in the two-dimensional case.

This Note presents the experimental results of surface pressure measurements obtained in the vicinity of an offset turbulent jet discharged from a rectangular outlet. The experimental apparatus described in Ref. 2 was appropriately modified to obtain data on the small surface pressures characteristic of offset three-dimensional jets. The effects of discharge Reynolds number Re_0, aspect ratio e, and offset distance h are examined. Details of the two-dimensional nature of surface pressure are described. A typical pressure contour map shown in Fig. 2 reveals a complex pattern not previously known.

Results

Extensive data were obtained on the surface pressure distribution P_s^* (x_1^*, x_3^*) for various values of the discharge Reynolds number, discharge aspect ratio, and offset distance. All lengths were nondimensionalized by division with the discharge height ($x_i=x_i^*/d^*$). In all tests, the nominal air temperature at the discharge was $-40°$C and the ambient temperature 31°C.

The effect of discharge Reynolds number Re_0 on the pressure coefficient $C_p(=P_s^*-P_\infty^*/\frac{1}{2}\rho_0^* U_0^{*2}$, where P_∞^* is the ambient pressure and ρ_0^* is density at the discharge) along the centerline (x_1, 0,0) was examined. It was noted that the general features of C_p are similar for the three Reynolds numbers considered ($Re_0=26{,}300$, 39,100, 55,400). Although little change in pressure is observed as Re_0 is increased from 26,300 to 39,100, pressure peaks are found to amplify significantly at $Re_0=55{,}400$.

Sudden expansion near the discharge results in subambient pressures that cause the jet to bend toward the surface, giving the negative values for C_p shown in Fig. 3. This behavior has also been observed in the preattachment region of two-dimensional offset jets[2-7] and is known as the Coanda effect. As the jet approaches the horizontal surface, it decelerates resulting in an increase in C_p, becoming positive at the reattachment position $x_1=x_A$ where the jet impinges on the surface. Beyond the reattachment point, the jet accelerates, remaining attached to the surface and eventually behaving as a wall jet. Correspondingly, the pressure coefficient drops, reaching negative values before increasing and asymptotically vanishing further downstream. This second region of subambient pressure is caused by the jet expansion and curvature over the thickening surface boundary layer in the wall jet region. Although the peaking of C_p downstream of reattachment and its subsequent drop have been observed in two-dimensional offset jets,[2-7] negative values downstream of x_A have not been previously reported. Careful examination of published surface pressure data shows that several investigators[2-5] terminated pressure measurements where they first reached the ambient level downstream of reattachment point x_A. Those who extended surface pressure measurements further downstream observed that the pressure remains at the ambient level.[6,7]

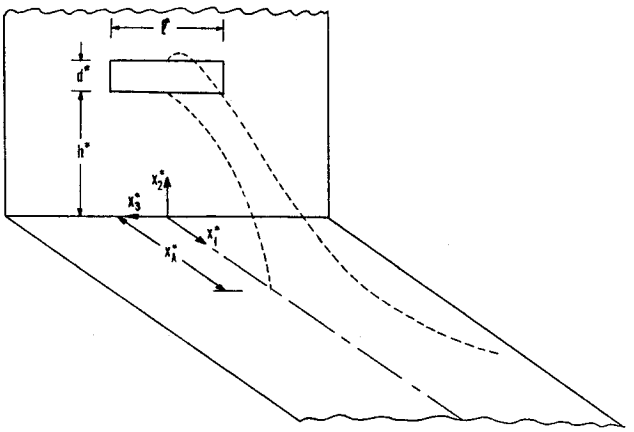

Fig. 1 Three-dimensional offset jet.

The negative/positive/negative feature of surface pressure coefficient at the centerline ($x_3=0$) was observed to characterize offset jets at various values of aspect ratio e and offset distance h, as shown in Figs. 2 and 3. This behavior presists at lateral distances x_3^* within the channel half-width, i.e., $x_3<\frac{1}{2}e$, as shown in Fig. 2. For a discharge with aspect ratio $e=0.25$, the outlet extends to $x_3=2$ in the lateral direction. Figure 2 suggests that $x_3=2$ appears to be the approximate limit for the negative/positive/negative behavior of surface pressure. At $x_3>2$, the peaks are attenuated in magnitude and no negative pressure develops downstream of the reattachment position. It is interesting to note that the maximum peaks do not occur at the centerline ($x_3=0$). The complex two-dimensional surface pressure distribution is illustrated in Fig. 2, where the isopressure curves are mapped.

Tests were carried out for various outlets to examine the effect of the discharge aspect ratio on the surface pressure. Figure 3 shows the centerline surface pressure distribution for $e=0$, 0.1, 0.25, and 0.44. To reveal the details of the pressure behavior downstream of the reattachment points, the pressure coefficient scale is magnified for $x_1>12$. The negative pressure peaks just downsteam of the discharge and the positive peaks after the reattachment are enhanced as the aspect ratio e is decreased. These peaks reach their maximum level for $e=0$, which corresponds to a two-dimensional slot jet. This case represents a slot of infinite length having no lateral entrainment. Experimentally, it is simulated by placing a vertical plate on each side of the outlet. The lower-pressure peaks associated with the three-dimensional outlets are attributed to lateral entrainment, which is absent in two-dimensional jets. Another consequence of lateral entrainment is the shifting upstream of pressure peaks as the aspect ratio is decreased, approaching its limit at $e=0$.

Careful measurements of pressure distribution downstream of the reattachment points show that subambient pressure readings were observed in this region for $e=0.1$, 0.25, and 0.44 (see Fig. 3). The magnitude of the pressure readings in this region is very small, typically $P_s^*-P_\infty^*\simeq 0.08$ mm H_2O; therefore, it can be mistakenly considered to be zero unless a sensitive pressure recording instrument is used.

The centerline axial pressure distribution corresponding to values of the offset distance h of 0.35-2.9 was also examined. The effect of h on the centerline pressure is qualitatively similar to that of the aspect ratio e shown in Fig. 3.

The maximum pressure coefficient $C_{p,\max}$ is plotted vs h in Fig. 4. Data for three-dimensional jets with aspect ratios $e=0.1$, 0.25, and 0.44 are compared with the limiting case of the two-dimensional slot jet ($e=0$). Striking differences between the two configurations are observed. For three-dimensional jets, $C_{p,\max}$ is significantly lower than that of two-dimensional slot jets. For example, at $h=0.5$, $C_{p,\max}$ for $e=0.44$ is an order of maginute lower than the two-dimensional value and at $h=3$ it is two orders of magnitude

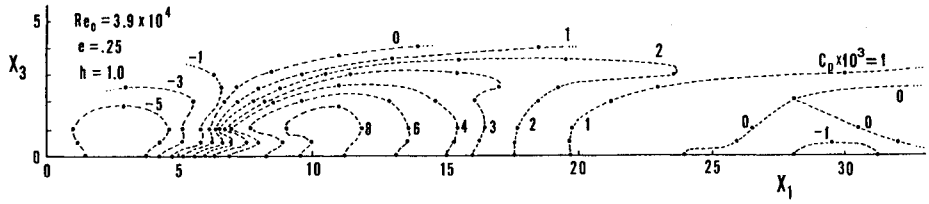

Fig. 2 Dimensionless surface isopressure map.

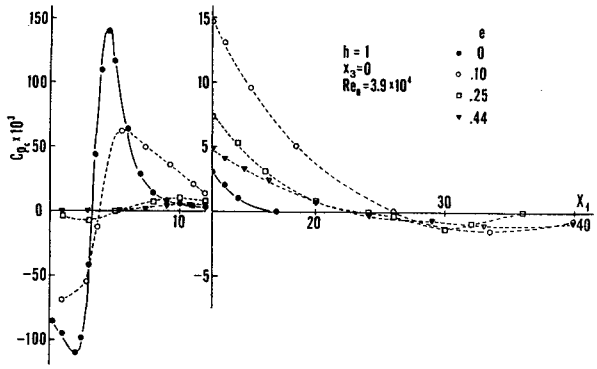

Fig. 3 Effect of discharge aspect ratio on centerline axial pressure distribution.

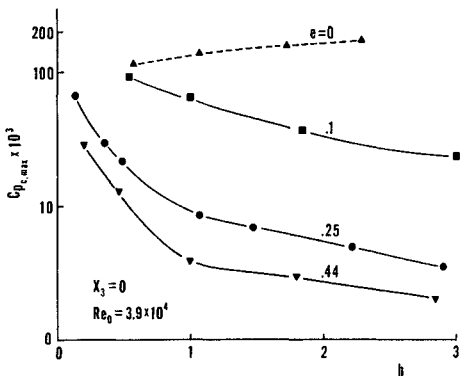

Fig. 4 Effect of offset distance on the maximum centerline pressure coefficient for two- and three-dimensional jets.

lower. Furthermore, a decrease in h brings about a decrease in $C_{p,\max}$ for two-dimensional jets, while it causes an increase in $C_{p,\max}$ for three-dimensional jets.

The behavior of surface pressure for small values of h requires careful consideration. For small values of the dimensional offset distance h^* compared to the discharge width ℓ^*, centerline surface pressure in the vicinity of the discharge should approach that of two-dimensional slot jets. Expressing this ratio in dimensionless form gives $h^*/\ell^* = eh$. Thus, two-dimensional behavior should be approached for $h \ll 1/e$. From this, it follows that the larger the aspect ratio, the smaller h must be to obtain pressure values of two-dimensional jets. This is clear in Fig. 4, which shows that $C_{p,\max}$ occurs in the vicinity of the discharge. For $e = 0.1$, $C_{p,\max}$ approaches its two-dimensional value at $h \simeq 0.5$. At this offset distance, $C_{p,\max}$ for $e = 0.44$ is still an order of magnitude lower than the value corresponding to two-dimensional jets. However, decreasing h further brings the value of $C_{p,\max}$ asymptotically closer to the jets two-dimensional level. In the limiting case of a wall jet ($h = 0$), the pressure throughout the jet is essentially equal to ambient value and, therefore, $C_p = C_{p,\max} \simeq 0$. Thus, at very small values of h (i.e., $h < 0.15$), the $C_{p,\max}$ curves for all aspect ratios should coalesce into as single curve along which $C_{p,\max}$ decreases as h is decreased (two-dimensional behavior) and vanishes at $h = 0$. It was not possible to verify this asymptotic behavior with the present experimental apparatus.

Conclusions

In general, surface pressure distribution for three-dimensional jets can differ signficantly from two-dimensional jets. However, the centerline surface pressure distribution for three-dimensional jets approaches that of two-dimensional jets at $h \ll 1/e$.

The negative/positive/negative feature of surface pressure coefficient was found to characterize three-dimensional offset jets. The negative surface pressure following reattachment is confined to lateral distances within the channel half-width, i.e., $x < 1/2e$. The negative pressure peaks just downstream of the discharge and the positive peaks after the reattachment points are enhanced as the aspect ratio and/or offset distance are decreased.

References

[1]Sacks, S., John, J. E. A., and Marks, C. H., "Interaction of a Three-Dimensional Fluid Jet with a Nearby Wall Boundary," *Proceedings of Thermal Pollution Analysis Conference*, Virginia Polytechnic Institute and State University, Blacksburg, 1974, pp. 96-117.

[2]Hoch, J. and Jiji, L. M., "Two-Dimensional Turbulent Offset Jet-Boundary Interaction," *Journal of Fluids Engineering*, Vol. 103, 1981, pp. 154-161.

[3]Bourque, C. and Newman, B. G., "Re-attachment of a Two-Dimensional Incompressible Jet to an Adjacent Flat Plate," *Aeronautical Quarterly*, Vol. 11, Aug. 1960, pp. 201-232.

[4]Newman, B. G., "The Deflection of Plane Jets by Adjacent Boundaries-Coanda Effect," *Boundary Layer and Flow Control*, Pergamon Press, London, 1961, p. 232.

[5]Parameswaran, V. and Alpay, S. A., "Studies on Reattaching Wall Jets," *Transactions of the CSME*, Vol. 3, No. 2, 1975, pp. 83-94.

[6]Rajaratnam, N. and Subramanya, K., "Plane Turbulent Reattached Wall Jets," *ASCE Journal of Hydraulics Division*, Vol. 94, 1968, pp. 95-112.

[7]Kumada, M., Mabuchi, I. and Oyakawa, K., "Studies in Heat Transfer to Turbulent Jets with Adjacent Boundaries, Third Report," *Bulletin of the JSME*, Vol. 16, Nov. 1973, pp. 1712-1722.

Transient Induced Drag

D. Weihs* and J. Katz†
NASA Ames Research Center, Moffet Field, California

Introduction

A FUNDAMENTAL problem of unsteady aerodynamics is the calculation of forces on a wing that is suddenly brought into motion at a constant speed. The simplest case (a two-dimensional, thin airfoil in an incompressible fluid) was

Received June 20, 1985; revision received Sept. 28, 1985. This paper is declared a work of the U.S. Government and is not subject to copyright protection in the United States.

*NRC Senior Research Associate; also Professor, Department of Aeronautical Engineering, Technion-Israel Institute of Technology, Haifa, Israel. Member AIAA.

†NRC Senior Research Associate. Member AIAA.